JSSS
Journal of Sensors
and Sensor Systems
Open Access

The magnetic field homogeneity of coils by means of the space harmonics suppression of the current density distribution

Christophe Coillot[1], Eric Nativel[2], Michel Zanca[1,3], and Christophe Goze-Bac[1]

[1]Laboratoire Charles Coulomb (L2C-UMR5221), BioNanoNMRI group, University of Montpellier,
Place Eugène Bataillon, 34095 Montpellier, France
[2]Institut d'Electronique et des Systèmes (IES-UMR5214), University of Montpellier,
Campus Saint-Priest, 34095 Montpellier, France
[3]Nuclear medicine, CMC Gui de Chauliac, University Hospital Montpellier,
34095 Montpellier, France

Correspondence to: Christophe Coillot (christophe_coillot@yahoo.fr)

Abstract. Electromagnetic coils are ubiquitously used in the modern world in motors, antennas, etc. In many applications (magnetic field coil calibration and nuclear magnetic resonance spectroscopy and imaging) there is a strong need for a homogeneous magnetic field. In this paper, we propose a simple modelling based on serial Fourier decomposition allowing the determination of the electrical conductor distribution to make the magnetic field homogeneous. The method is valid both for plane and axisymmetric geometries. The method allows the retrieval of the classical configurations of saddle coil for the plane geometry and Helmholtz coil for the axisymmetric one. The method is generalized for any number of electrical conductors and brings the perspective of new homogeneous magnetic resonance imaging (MRI) coil configuration.

1 Introduction

Electrical coils have had a long history since the pioneer works of Ampere and Tesla. Their emergence comes probably from their ability to extend the fascinating properties of the magnetized matter by modulating their behaviour by means of electrical currents. Unfortunately, the magnetic field produced by electrical coils exhibits a strong dependance on the distance compared to the coil, since the magnetic field produced by a coil vanishes when going away from the coil plane, while numerous applications require a homogeneous one. This is the concern of nuclear magnetic resonance spectroscopy (NMR) and magnetic resonance imaging (MRI) where the homogeneity of coils is crucial for the static B_0 magnetic field but also important for the radiofrequency (RF) coil, which produces the B_1 RF field to excite and to detect the nuclear spin induction. This MRI coil homogeneity, which has guided the present work, remains a major issue for the MRI experiment (Mispelter et al., 2006). Usu-

ally, MRI coil length should be smaller than a fraction of the wavelength (1/20) at the frequency of interest. When it is not the case, MRI coil should be segmented (Mispelter et al., 2006) to ensure that quasi-static magnetic field hypothesis is suitable. Our work will be examined based on this hypothesis. We will consider the 1 and 10 % homogeneity defined as the fraction of coil diameter, where the magnetic field intensity remains, respectively, within 1 and 10 % of its maximum value.

2 Homogeneous magnetic field coils: the cosine current distribution theorem

It was assumed by Bolinger et al. (1988) that a cosine current distribution for both a spherical coil and a coil constituted by parallel conductors placed on a circle allows them to approach an ideal magnetic field homogeneity. We will try to
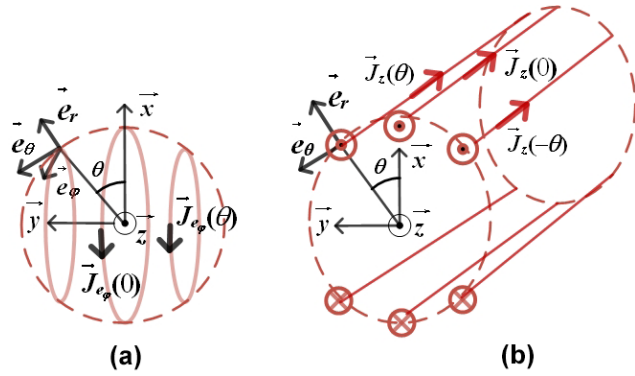
Figure 1. Current density distribution: **(a)** axisymmetric geometry in spherical coordinates, **(b)** plane geometry (infinite in z direction) in cylindrical coordinates. We adopt a unique angle notation for the two problems by substituting the usual φ (in the cylindrical coordinates) by θ.

Figure 2. Representation of the magnetic field components $\mathbf{H}$, $\mathbf{H}_r$ and $\mathbf{H}_\theta$ in the cartesian and cylindrical coordinates. Spherical coordinate representation is equivalent to the cylindrical one in a revolution near.

understand, in the following, the origin of this current density distribution theorem.

The cosine distribution can be deduced from the Maxwell–Ampere equation (Eq. 1), which basically links the magnetic field $\mathbf{H}$ and the current density $\mathbf{J}$.

$$\nabla \times \mathbf{H} = \mathbf{J} \tag{1}$$

We have to determine the current density component on the circumference of a R radius, along z, for cylindrical coordinates (see Fig. 1b), or along e_φ, for spherical coordinates (see Fig. 1a).

Since the current density has only a component along z (following the Bolinger et al., 1988, case study), in cylindrical coordinates, Maxwell–Ampere equation becomes

$$\frac{1}{r}\left(\frac{\partial(r H_\varphi)}{\partial r} - \frac{\partial H_r}{\partial \varphi}\right) = J_z(\theta, r). \tag{2}$$

In spherical coordinates, Maxwell–Ampere equation becomes

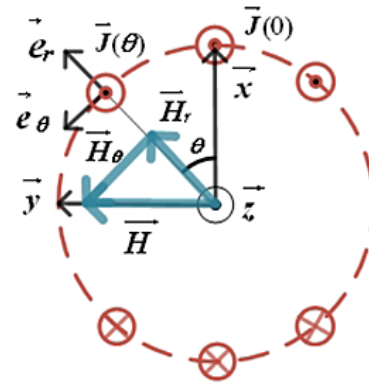$$\frac{1}{r}\left(\frac{\partial(r H_\theta)}{\partial r} - \frac{\partial H_r}{\partial \theta}\right) = J_{e_\varphi}(\theta, r). \tag{3}$$

Due to the equivalence between these two equations we will adopt a unique angle notation by substituting φ (in the cylindrical coordinates) with θ. Consequently, Eq. (2) is replaced by

$$\frac{1}{r}\left(\frac{\partial(r H_\theta)}{\partial r} - \frac{\partial H_r}{\partial \theta}\right) = J_z(\theta, r). \tag{4}$$

Next, by assuming a constant magnitude of the magnetic field ($\mathbf{H}$, as depicted in Fig. 2), we get $H_r^2 + H_\theta^2 = H^2$, while the x and y components of $\mathbf{H}$ in cartesian coordinates are related to the ones in cylindrical (and spherical) coordinates:

$$\begin{cases} \mathbf{H} \cdot \mathbf{x} = H_r\cos(\theta) - H_\theta\sin(\theta) \\ \mathbf{H} \cdot \mathbf{y} = H_r\sin(\theta) + H_\theta\cos(\theta). \end{cases}$$

Then, by assuming a given direction of the magnetic field, for instance $\mathbf{H} \cdot \mathbf{x} = 0$ (see Fig. 2), we deduce $H_r\cos(\theta) = H_\theta\sin(\theta)$ and consequently $H_r = H\sin(\theta)$.

By solving Maxwell–Ampere equation at $r = R$ (the term $\frac{\partial(r H_\theta)}{\partial r}$ vanishes) Eqs. (3) and (4) become, respectively, Eqs. (5) and (6):

$$-\frac{1}{R}\frac{\partial H_r}{\partial \theta} = J_{e_\varphi}(\theta) \tag{5}$$

$$-\frac{1}{R}\frac{\partial H_r}{\partial \theta} = J_z(\theta). \tag{6}$$

Thus, we obtain the condition that must be fulfilled by the current density to produce a homogeneous magnetic field for coils of revolution with axisymmetric geometry (Fig. 1a) and infinite plane geometry (Fig. 1b), given respectively by Eqs. (7) and (8):

$$\mathbf{J}_{e_\varphi}(\theta) = J_0\cos(\theta)e_\varphi \tag{7}$$

$$\mathbf{J}_z(\theta) = J_0\cos(\theta)z, \tag{8}$$

where $J_0 = -\frac{1}{R}H$.

Lastly, the simulation performed on a finite-element software, which allows the confirmation of this rule, illustrates the perfect homogeneity inside the coil obtained both for axisymmetric revolution geometry and 2-D plane when the magnitude of the current density is cosinusoidal along the circumference of a circle (see Fig. 3). In both cases, the current density direction is normal to the figure.
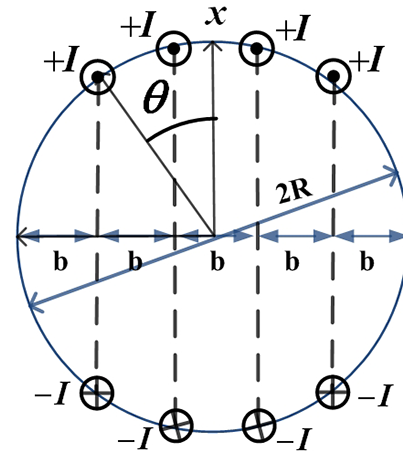
3　The cosine coils: a brief review

The spherical coil configuration was initially proposed to enhance the Helmholtz coil homogeneity for nuclear research (Clarck, 1938). Later, it was used to build a proton magnetometer (Everett and Osemeikian, 1966). In this context it was required to produce a homogeneous magnetic field. For
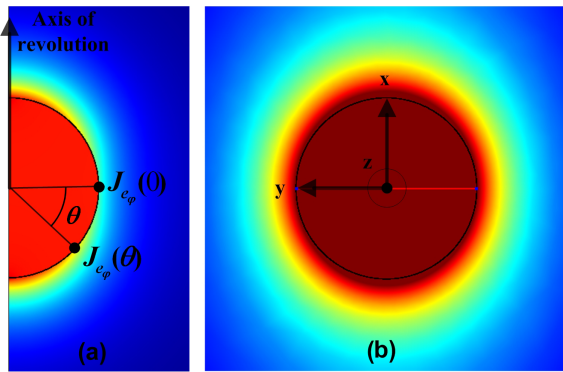
Figure 3. Magnetic field magnitude distribution of the ideal homogeneous coil (assuming $\cos(\theta)$ distribution of the current density along the circumference) performed on a numerical finite-element software: **(a)** case of a solid of revolution and **(b)** case of a 2-D plane infinite (along z) geometry. The colour scale is related to the magnitude of the magnetic field. The homogeneity of the colour is related to the homogeneity of the magnetic field.

Figure 4. Bolinger's coil: the turns, distributed along the circumference (placed around the cylinder at angles θ (NB the complementary angle Φ was used in Bolinger's paper)), are equally spaced projected along the diameter ($b = 2R/(2N+1)$).

this purpose Everett tried to approach the ideal cosine current density distribution, and the authors suggested to approach the ideal sphere coil by placing N equally spaced turns (on the diameter projection) separated by a distance b, each turn being flown by the same current (see Fig. 4). The main variable of the problem was the parameterization (through a parameter p) of the last turn position, namely pb. Then sophisticated analytic calculations were performed to get the optimum p value ($0 < p < 1$), with respect to a magnetic field homogeneity criterion. Finally the coil, let us call it Everett's coil, was constructed but the conclusion concerning the efficiency was mitigated. Surprisingly, the alternative solution to produce a cosine current distribution, namely by adjusting the current density in the conductors of the sphere coil, was not evoked.

Later on, in the field of MRI coils, there were numerous efforts to enhance the homogeneity of the coil. The saddle coil, which is the extruded plane version of the Helmholtz coil, was generalized because of its convenience with respect to the NMR experience (Hoult and Richards, 1976). A very important enhancement of the saddle coil was then proposed by Hayes et al. (1985) through the birdcage resonator. This famous MRI coil consists in multiple conductors equally spaced (on the angular point of view). Capacitors are used to produce a phase shift of the current along the circumference to approach the ideal cosine distribution (as given by Eq. 8). The Bolinger idea was to apply Everett's coil strategy to the saddle coil (Bolinger et al., 1988). However, Bolinger simplified the original problem by assuming N equally spaced conductors, without the p parameter. A homogenous image about four-fifths of the internal volume of the coil was reported. Nevertheless, a quantitative and relevant method to quantify homogeneity of MRI coils by means of field histogram proposed by Yang et al. (1994) has high-

lighted the disappointing homogeneity reached by Bolinger's coil.

On the other hand, an improvement of the birdcage was invented by Harpen (1991), who proposed a spherical RF coil where the turns were equally spaced (by equal angle). The cosine current distribution (as given by Eq. 7) was reached by an adequate distribution of the capacitances: $C(\theta) = C_0/\sin(\theta)$.

Lastly the four coils proposed by Hoult and Deslaurier (1990) gave a significant improvement of the Helmholtz coil, at the expense of sophisticated computation, where both conductor locations and current flowing through the coils are computed to improve the homogeneity. The four coils require a specific ratio between the current flowing into the inner and outer pairs of conductor.

4 The Bolinger cosine coil paradox

As proposed initially by Clarck (1938) and Everett and Osemeikhian (1966), for axisymmetric revolution, and revisited by Bolinger, for plane geometry, the cosine coil is such that wire positions are found by a geometric construction where intervals of equal length along the diameter are projected onto the circumference (Bolinger et al., 1988), as shown in Fig. 4. Thus, for N turns (or conductors), the space between turns is given by $b = 2R/(N+1)$ while the position of the nth turn on the y axis is given by $y(n\text{th}) = n\text{th}b + R/N$.

Let us first consider the simplest coil obeying this rule: the two-turn coil. By applying the cosine coil rule as proposed by Bolinger, it follows that distance between turns should be $2R/3$, so the angle θ (with respect to x axis, as defined in Fig. 4) is $\approx 19.5°$. Surprisingly, this is far from the classical saddle coil condition (namely $\theta = 30°$). That strangeness led us to investigate the rule to obtain a cosine current repartition.
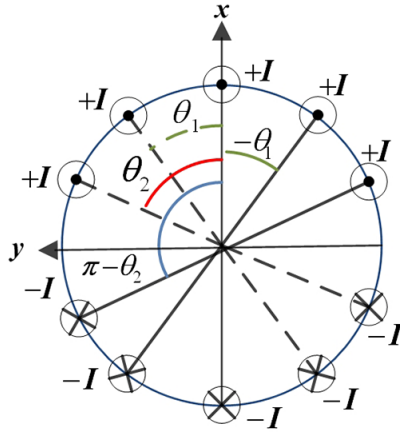
Figure 5. Electrical conductors of unknown angular positions (θ), flown by the same current I, distributed along the circumference.

5 Spatial harmonics of the current distribution produced by the discrete conductors coil

We now go back to the original problem: how to distribute the electrical conductors, flown by the same current, along the circumference to get a homogeneous magnetic field inside the coil.

The problem, as illustrated in Fig. 5, is equivalent to seeking the optimum angle position (θ) of each conductor.

Let us now represent the current distribution of the coil of Fig. 5 in a more convenient way where electrical conductors are represented by means of Dirac distributions (see Fig. 6). To this end, we use a one-dimensional Dirac distribution (δ) as a function of the angle θ so that δ has the unit rad^{-1} and such as $\int_0^{2\pi} \delta(\theta) d\theta = 1$. Next, we consider N pairs of conductors infinitely thin, flown by the same current I, and the nth conductor is defined by its angle position θ_n (Fig. 6). For such a conductor, we use a current density distribution $j(\theta) = \pm I \delta(\theta - \theta_n)$ in A/rad, where the $\pm$ sign depends on the direction of the current density flow. Finally, the current density distribution of the coil of Fig. 5 is expressed as

$$j(\theta) = I\delta(\theta) - I\delta(\theta - \pi) + \Sigma_{n=1}^{N}(I\delta(\theta - \theta_n) + I\delta(\theta + \theta_n)$$
$$- I\delta((\theta - \theta_n) - \pi) - I\delta((\theta + \theta_n) - \pi)). \quad (9)$$

The current density distribution is an even function, and the terms $\delta(\theta)$ and $\delta(\theta - \pi)$ are related to the central coil. In the case of an even-turn number (namely without the central conductor at $x = 0$), these terms can be omitted. Next, due to the symmetries of the current density distribution (see Fig. 6), the calculation of the Fourier series ($a_{(2k-1)}$) coefficients is simplified and we get k as an integer:

$$a_{(2k-1)} = \frac{2}{\pi} \int_{-\pi/2}^{\pi/2} j(\theta)\cos((2k-1)\theta)d\theta. \quad (10)$$
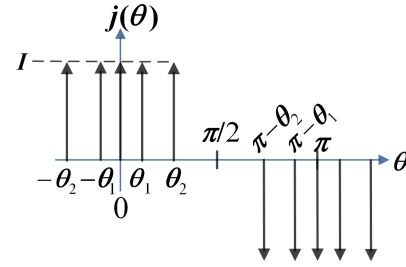
Figure 6. Representation of the space current density distribution.

For the coils having a central conductor we get k as an integer:

$$a_{(2k-1)\text{odd}} = \frac{2I}{\pi} \Sigma_{n=1}^{N}(1 + 2\cos((2k-1)\theta_n)), \quad (11)$$

and the current density function is expressed as

$$j(\theta)_{\text{odd}} = \Sigma_{k=1}^{\infty}\left(\Sigma_{n=1}^{N} \frac{2I}{\pi}(1 + 2\cos((2k-1)\theta_n))\right)$$
$$\times \cos((2k-1)\theta). \quad (12)$$

For the coils without the central conductor we get

$$a_{(2k-1)\text{even}} = \frac{4I}{\pi} \Sigma_{n=1}^{N}\cos((2k-1)\theta_n), \quad (13)$$

and the current density function is expressed as

$$j(\theta)_{\text{even}} = \Sigma_{k=1}^{\infty}\left(\Sigma_{n=1}^{N} \frac{4I}{\pi}\cos((2k-1)\theta_n)\right)$$
$$\times \cos((2k-1)\theta). \quad (14)$$

Equations (12) and (14) will be the basis of the space harmonic suppression (SHS) method. The Fourier series decomposition has an infinite number of harmonics. Each harmonic can be cancelled by means of a supplementary conductor. To reach a perfect homogeneity all the harmonics should be cancelled and consequently an infinite number of conductors would be required. In such a "theoretical" case, the infinite discrete conductor distribution will be equivalent to the perfect homogeneous coil (i.e. with an ideal cosine current density distribution) whose simulation result is reported in Fig. 3.

In the following, we will perform a case study for two, three, four and six turns by means of a magnetostatic finite-element numerical simulation for the two kinds of cosine coils: the cosine coil obeying Everett–Bolinger rule and the cosine coil obtained by the SHS method, referred to as SHS coil. The simulation results will be presented for the infinite plane geometry, but they are also valid for the axisymmetric geometry.

Table 1. Three-turn infinite plane coil homogeneity: comparison between the Maxwell and the three-turn SHS coils. The 1 and 10 % homogeneity are defined as the fraction of the coil diameter where the magnetic field intensity remains, respectively, within 1 and 10 % of its maximum value.

Coil type	Maxwell coil	Three-turn SHS
1 % homogeneity	0.22	0.40
10 % homogeneity	0.63	0.68

Table 2. Three-turn axisymmetric coil homogeneity: comparison between the Maxwell and the three-turn SHS coils.

Coil type	Maxwell coil	three-turn SHS
1 % homogeneity	0.41	0.52
10 % homogeneity	0.68	0.72

Table 3. Four-turn axisymmetric coil homogeneity: comparison between the Hoult–Deslauriers coil and the four-turn SHS coils.

Coil type	Hoult–Deslauriers coil	Four-turn SHS
1 % homogeneity	0.56	0.51
10 % homogeneity	0.78	0.77

5.1 Two-turn coil

Let us study the case of the two-turn coil (i.e. one pair of turns: $N = 1$). In such a case, the condition to cancel the first harmonic ($k = 2$), from Eq. (14), is expressed as

$$\cos(3\theta_1) = 0, \tag{15}$$

which obviously leads to $\theta_1 = \pi/6$, namely the Helmholtz condition for the axisymmetric problem and the saddle coil condition for the plane geometry (Hoult and Richards, 1976). On the other hand the Bolinger cosine coil condition (the turns are equally spaced projected along the diameter) leads to $b = 2R/3$. Under this condition the obtained homogeneity is very poor (see Fig. 7).

5.2 Three-turn coil: comparison with Maxwell coil

The Maxwell coil is a famous homogeneous coil with odd turns (three turns). This coil is defined by $\cos(\theta) = \sqrt{4/7}$ ($\sim$ 40.89°) and $I/I_0 = 49/64$, where I_0 is the current into the central coil while I is the current on the lateral coils.

Let us now study the three-turn SHS coil. Thus, we just have to solve $1 + 2\cos(3\theta_1) = 0$, which leads to $\theta = \pm\frac{4\pi}{9} + m\frac{2\pi}{3}$, where m is an integer. It is noticeable that the first angle solution ($\theta = \frac{4\pi}{9}$) leads to a good magnetic field homogeneity (the simulation results are not presented here) while it leads to a very poor efficiency coil because of the reduced magnitude of the fundamental contribution (namely the term $1 + 2\cos(\theta_1) = 0$). Thus, each solution of θ must be evaluated with respect to the fundamental magnitude. In this case, the solution $\theta = \frac{16\pi}{9}$ ($= 40°$) leads to the higher value of the fundamental. Finally, let us compare the three-turn SHS coil to the Maxwell coil. From numerical simulation, we can extract the 1 and 10 % homogeneity ranges. First, in the context of an infinite plane geometry coil (see Table 1), the three-turn SHS coil exhibits a slightly better 1 and 10 % homogeneity than the Maxwell one.

Second, in the context of an axisymmetric geometry, which corresponds to the validity domain of the Maxwell coil, the 1 and 10 % homogeneity of the SHS, as summarized by Table 2, are better. Nevertheless, the three-turn SHS coils exhibit small fluctuations of the magnetic field in the centre part of the coil (< 1 %) while it is rigorously homogeneous for the Maxwell coil. However, as emphasized by Mispelter

et al. (2006), the RF MRI coil homogeneity is not extremely stringent, typically about ± 5 %.

5.3 Four-turn coil

Let us now study the case of two pairs of turns (i.e. $N = 2$). The conditions to cancel the first and second harmonics are

$$\cos(3\theta_1) + \cos(3\theta_2) = 0$$
$$\cos(5\theta_1) + \cos(5\theta_2) = 0, \tag{16}$$

which leads to $\theta_1 = \pi/15$ and $\theta_2 = 4\pi/15$. On the one hand the Bolinger cosine coil condition is $b = 2R/5$; its homogeneity is slightly improved (with respect to the two-turn Bolinger coil) but remains still far from the one obtained for four-turn SHS coil. On the other hand, it is interesting to notice that the Hoult and Deslauriers coil condition (see Hoult and Deslaurier, 1990) for the axisymmetric problem led to angles $\epsilon = 0.699$ and $\psi = 1.282$ (we report here the angle notation used in Hoult and Deslauriers's paper) defined with respect to the x axis (see Fig. 7), which becomes the following in our notation context: $\psi' = \pi/2 - \psi = 0.288 \approx \theta_1$ and $\epsilon' = \pi/2 - \epsilon = 0.871 \approx \theta_2$, which are close to the values we obtained for the SHS. However a supplementary condition on the current flowing in each pair of turns ($I_2/I_1 = 0.682$) was also required by the four-coil configuration to achieve very high homogeneity (suppression of the sixth-order component of the Legendre polynomials series decomposition of the magnetic field) while the SHS coil assumed identical current flowing through the conductors (which is easier to reach in practice). Practically both the 1 and 10 % homogeneity of the Hoult and Deslauriers coil are slightly better than the four-turn SHS coil (see Table 3). It suggests that the use of a supplementary variable (current ratio) to suppress harmonic is efficient.

Table 4. Coil homogeneity efficiency summary (in the plane geometry): comparison between the Everett–Bolinger coils and SHS coils.

Bolinger coil	Two turns	Four turns	Six turns
1 % homogeneity	0.1	0.20	0.24
10 % homogeneity	0.36	0.5	0.59

SHS coil	Two turns	Four turns	Six turns
1 % homogeneity	0.33	0.51	0.61
10 % homogeneity	0.58	0.77	0.83

5.4 Six-turn coil

Let us now study the case $N = 3$. In such a case, the condition to cancel the harmonics are expressed as

$$\cos(3\theta_1) + \cos(3\theta_2) + \cos(3\theta_3) = 0$$
$$\cos(5\theta_1) + \cos(5\theta_2) + \cos(5\theta_3) = 0 \qquad (17)$$
$$\cos(7\theta_1) + \cos(7\theta_2) + \cos(7\theta_3) = 0.$$

The angle solutions (in radians) of Eq. (17) are easily found by means of a numerical minimization algorithm: [$\theta_1 = 0.2035, \theta_2 = 0.4537, \theta_3 = 0.977$]. A Newton algorithm (similar to the one described in Coillot et al., 2007) was used, but a genetic algorithm would be best suited for a higher turn number. On the other hand, the angle position of the conductors of the Everett–Bolinger six-turn coil will be [$\theta_1^{EB} = 0.143, \theta_2^{EB} = 0.443, \theta_3^{EB} = 0.796$]. Here again, the homogeneity of the Everett–Bolinger coil, as depicted in Fig. 7, is far from the one obtained by the SHS coil. One can notice that the SHS coil will not obey the Everett cosine coil rule (even if the last turn position is used as a variable of the b distance), since the positions on the x axis of the first and second turns of the six-turn SHS coil (respectively $\sin(\theta_1) = 0.202$ and $\sin(\theta_2) = 0.438$) are not at multiple distances ($b/2$ and $b + b/2$).

All the presented results are mostly qualitative and a quantitative study on the homogeneity should be performed to appreciate the benefit of the proposed method. To this aim, on the one hand we compare, in Fig. 8, the magnetic field profile along y axis for the different coils. On the other hand, we propose to perform quantitative comparisons by means of two homogeneity criteria: the 10 % homogeneity criterion (which is sufficient for RF MRI coil; Mispelter et al., 2006) and the 1 % criterion (which is well adapted for stringent design as for the magnetic field calibration devices). Table 4 summarizes the obtained homogeneity for the two types of coils.

5.5 Generalization of the method for even-turn coil

In the context of an N-turn coil pairs, we will have to determine the N angles satisfying the N harmonic suppression, as given by the set of N equations:
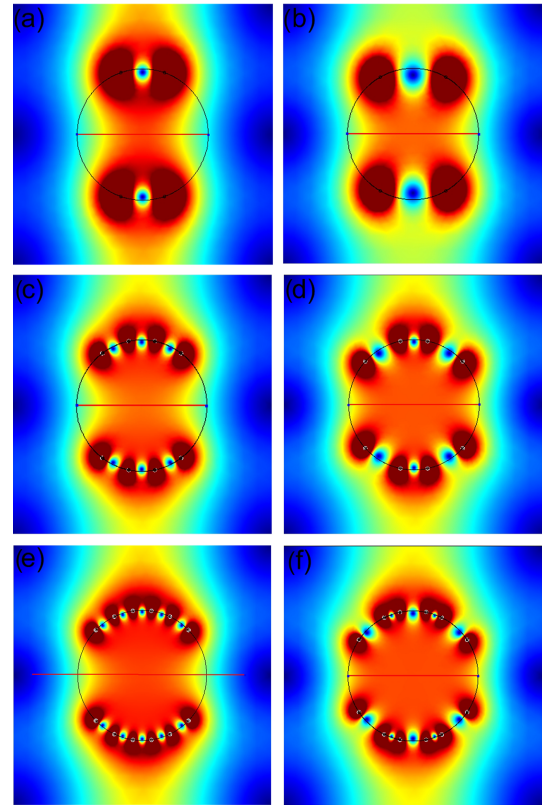
Figure 7. Magnetic field homogeneity of the Everett–Bolinger coil: **(a)**, **(c)** and **(e)**, respectively, for two, four and six turns. The SHS coil: **(b)**, **(d)** and **(f)**, respectively, for two, four and six turns.
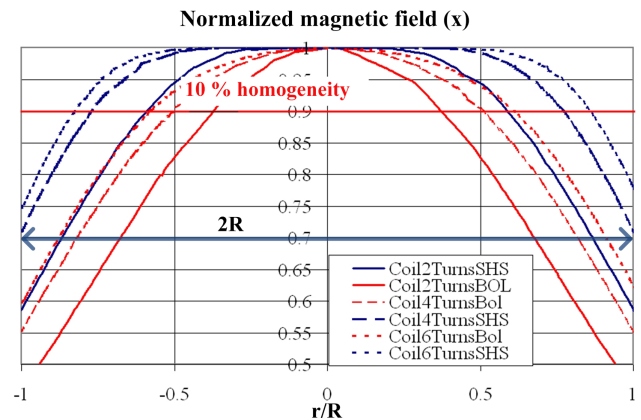
Figure 8. Magnetic field homogeneity profile on the x axis, comparison between Everett–Bolinger coil and SHS coil for two, four and six turns.

$$\Sigma_{n=1}^{N}(\cos(3\theta_n)) = 0 \, (k = 1)$$

$$\dots$$

$$\Sigma_{n=1}^{N}(\cos((2j - 1)\theta_n)) = 0 \, (k = j) \qquad (18)$$

$$\dots$$

$$\Sigma_{n=1}^{N}(\cos((2N - 1)\theta_n)) = 0 \, (k = N).$$

5.6 Generalization of the method for odd-turn coil

In the context of an N-turn coil pairs plus the central conductor, we will have to determine the N angles satisfying to the N harmonic suppression, as given by a set of N equations:

$$1 + \Sigma_{n=1}^{N}(\cos(3\theta_3)) = 0 (k = 1)$$
$$\cdots$$
$$1 + \Sigma_{n=1}^{N}(\cos((2j-1)\theta_n)) = 0 (k = j) \qquad (19)$$
$$\cdots$$
$$1 + \Sigma_{n=1}^{N}(\cos((2N-1)\theta_n)) = 0 (k = N).$$

6 Discussion

The proposed method neglects the real size of the conductor. Thus, the accuracy of the method could be enhanced by taking into account the real conductor size in the Fourier series decomposition. Nevertheless, at high frequency, where skin effect is not negligible, the occurrence of the proximity effect could affect the current distribution in conductors and modify the homogeneity. Lastly, the method is also applicable for the odd coil turns case even if we have focused on an even one. However, it is noticeable that simulation results between extruded geometry and axisymmetric one are slightly different.

As an alternative method, we could consider minimizing all the harmonic contribution, but it seems that the harmonic by harmonic minimization is much more reliable. The reason probably comes from the fact that the Dirac conductor is not real and the contribution of the high-order harmonics is not negligible while, in practice, the high space harmonics effect should decrease rapidly. The superiority of the Hoult and Deslauriers coil, using a supplementary variable (namely the current ratio between coils), could inspire an extension of the SHS method).

In the context of odd coil, we have seen in a case study that, at the same time that the harmonics are minimized, we should maximize the fundamental. So, rigorously, each solution should satisfy both to the suppression of harmonics and the maximization of the fundamental.

One could ask what the benefits or disadvantages of an enhanced homogeneity would be. Let us consider the case of a calibration coil. For a given homogeneous volume the radius of the coil can be reduced. It follows that its mass and cost will be reduced too. This benefit was pointed out by Everett and Osemeikhian (1966).

Finally, in the context of MRI coils, the resulting image homogeneity will depend on (as discussed in Coillot et al., 2016) the RF coil configuration (emitter, transceiver, or both emitter and a transceiver), the magnetic field homogeneity inherent to the coil geometry and the type of running MRI sequence.

7 Conclusions

The SHS is demonstrated to be an efficient analytic method to determine the conductor distribution to enhance the coil homogeneity. It should be noticed that a finite-element-method software analysis combined to an optimization algorithm could be performed as an alternative method to determine the angle position, at the expense of a strong programming effort and a long CPU time. The initial idea of Everett, for the axisymmetric coil, and Bolinger, for extruded geometry, to approach the cosine current density distribution by allocating the conductor along a circle circumference was luminous. Nevertheless, the intuitive rule they proposed to build their coils was not really relevant to improving homogeneity. The SHS method allows the exact and easy determination of the position of the conductor even for a high turn number. That opens up a new perspective in the field of MRI, especially by revisiting the Bolinger cosine coil.

References

Bolinger, L., Prammer, M. G., and Leigh, J. S.: A Multiple-Frequency Coil with a Highly Uniform B_1 Field, J. Magn. Reson., 81, 162–166, 1988.

Clark, J. W.: A new method for obtaining a uniform magnetic field, Rev. Sci. Instrum., 9, 320–322, 1938.

Coillot, C., Moutoussamy, J., Leroy, P., Chanteur, G., and Roux, A.: Improvements on the Design of Search Coil Magnetometer for Space Experiments, Sens. Lett., 5, 167–170, 2007.

Coillot, C., Sidiboulenouar, R., Nativel, E., Zanca, M., Alibert, E., Cardoso, M., Saintmartin, G., Noristani, H., Lonjon, N., Lecorre, M., Perrin, F., and Goze-Bac, C.: Signal modeling of an MRI ribbon solenoid coil dedicated to spinal cord injury investigations, J. Sens. Sens. Syst., 5, 137–145, doi:10.5194/jsss-5-137-2016, 2016.

Everett, J. E. and Osemeikhian, J. E.: Spherical coils for uniform magnetic fields, J. Sci. Instrum., 43, 470–474, 1966.

Harpen, M. D.: The Spherical Birdcage Resonator, J. Magn. Reson., 94, 550–556, 1991.

Hayes, C. E., Edeutein, W. A., Schenck, J. F., Mueller, O. M., and Eash, M.: An Efficient Highly Homogeneous Radiofrequency Coil for Whole-Body NMR Imaging at 1.5T, J. Magn. Reson., 63, 622–628, 1985.

Hoult, D. I. and Deslaurier, A.: High-Sensitivity and High B_1 Homogeneity Probe for Quantitation of Metabolites, Magn. Reson. Med., 16, 411–417, 1990.

Hoult, D. I. and Richards, R. E.: The signal-to-noise ratio of the nuclear magnetic resonance experiment, J. Magn. Reson., 24, 71–85, 1976.

Maxwell coil: https://en.wikipedia.org/wiki/Maxwell_coil, last access: 18 November 2016.

Mispelter, J., Lupu, M., and Briguet, A.: NMR probehads for biophysical and biomedical experiments: theoretical principles and practical guidelines, Imperial College Press, 301–435, 2006.

Yang, Q. X., Li, S. H., and Smith, M. B.: Method for Evaluating the Magnetic Field Homogeneity of a Radiofrequency Coil by Its Field Histogram, J. Magn. Reson., 108, 1–8, 1994.